MAPS OF HCO^+ EMISSION IN C/1995 O1 (HALE–BOPP)

M. WOMACK* and A. HOMICH
Department of Physics and Astronomy, St. Cloud State University, St. Cloud, MN 56301-4498, USA
(E-mail: Womack@r2d2.stcloudstate.edu)*

M. C. FESTOU
Observatoire Midi Pyrénées, 14 avenue E. Belin, F-31400, Toulouse, France

J. MANGUM
National Radio Astronomy Observatory, Tucson, AZ, USA

W. T. UHL
Yale University, USA

S. A. STERN
Southwest Research Institute, 1050 Walnut Street, No. 426, Boulder, CO 80302, USA

(Received 4 February 1998; Accepted 29 April 1998)

Abstract. On-the-Fly maps of emission from the HCO^+ J = 3-2 transition at 267.6 GHz were obtained of C/1995 O1 (Hale–Bopp) on 1997 Mar 15.6 UT using the NRAO 12-m telescope with high spatial resolution. Unlike the relatively symmetric and centralized maps of the neutral species CO, HCN and H_2CO, the spatial extent of HCO^+ emission is very diffuse with a complex structure characterized by at least two physically different regions. The bulk of the HCO^+ emission peaks in intensity ∼175,000 km anti-sunward from the nuclear position. This peak emission does not fall directly along the anti-sunward direction, but is rotated by ∼10 degrees toward the east from the anti-sunward direction. A substantial void, or decrease, of HCO^+ emission is observed within ∼ 55,000 km of the nucleus. The HCO^+ emission in this void is roughly half the intensity of the emission observed 100,000 km away. This decrease of HCO^+ emission near the nucleus may indicate that production or excitation of HCO^+ is inhibited, or perhaps that HCO^+ is easily destroyed in the inner coma, especially within ∼50,000 km of the nucleus. This void roughly coincides with the approximate location and size of the so-called "diamagnetic cavity" in the coma and may mark a significant transition region in the inner coma of Hale–Bopp.

Keywords: Comet Hale–Bopp, ions, HCO^+

1. Introduction

Measuring the spatial distribution of molecular ions in comae is a valuable way to study the complex physical interactions between molecules and the solar wind (e.g., Galeev et al., 1989; Ip, 1989; Cravens, 1991; Larson et al., 1997; Gombosi et al., 1997–1999). Recently, a new cometary ion, HCO^+, was detected which provides additional opportunities for probing these effects. HCO^+ was first observed in a comet via the ion's J = 1–0 transition at 89 GHz in C/1995 O1 when the comet was ∼ 1.2 AU from the Sun (Veal et al., 1997). The original data showed that

HCO^+ linewidths were asymmetric with redward wings and line centers significantly redshifted with respect to the comet nucleus velocity. Thus, HCO^+ emission exhibited asymmetric behavior worth exploring further with mapping techniques. The observed line radiation temperature of HCO^+ in comet Hale–Bopp was strong enough so that we could use the technique of On the Fly (OTF) mapping to study the spatial distribution of HCO^+ with a relatively high sampling of 6 arcsec over an extent of several arcminutes, while still retaining the velocity information of the ion. The goal was to obtain maps of HCO^+ emission corresponding to different radial velocities in the coma. Here we provide high signal-to-noise and moderately high angular resolution millimeter-wavelength maps of the HCO^+ J = 3-2 emission obtained with the NRAO 12-m telescope when the comet was near perihelion.

2. Observations and Reductions

The data were obtained on UT 1997 March 15.6 with the NRAO 12-m telescope in the On-the-Fly (OTF) spectral mode. The single dish antenna was slewed back and forth across the sky to cover a 6.4 $\times$ 6.4 arcmin patch of sky, and spectra were recorded every 0.10 seconds. We scanned alternately in RA and Dec to minimize any scanning artifacts. A total of seven maps were obtained for a total of 7.9 hours of integration time. The data were obtained with spectral resolutions of 500 kHz and 1 MHz with the filterbanks and 391 kHz with the hybrid spectrometer. The pointing and focus were checked after each map to minimize instrumental differences in the data. The seven OTF maps were trimmed at the edges to remove regions with poor sampling and examined to search for short-term (i.e., hours) variations in the molecular ion's spatial distribution. After no significant variation was detected, the seven maps were summed to form a spectral datacube covering over 8 hours in time.

During the time of observations, the comet had a heliocentric distance of 0.960 AU and geocentric distance of 1.33 AU. The HPBW angular resolution of the beam is 23 arcsec and the sample size is 6 arcsec providing an effective spatial resolution of 22,187 km and an effective sample size of 5788 km on the plane of the sky at the comet's distance. The comet's topocentric radial velocity was -9.8 km s^{-1} at the beginning of the mapping, which corresponds to emission between panels E and F. The phase angle of the comet was 48.0 degrees and and position angle of the Sun was 168.3 degrees.

3. Results and Discussion

The HCO^+ linewidths are measured to be broad (FWHM $\sim$5 km s^{-1}) and redshifted from the nuclear velocity by 1–2 km s^{-1}. The broad linewidth is expected

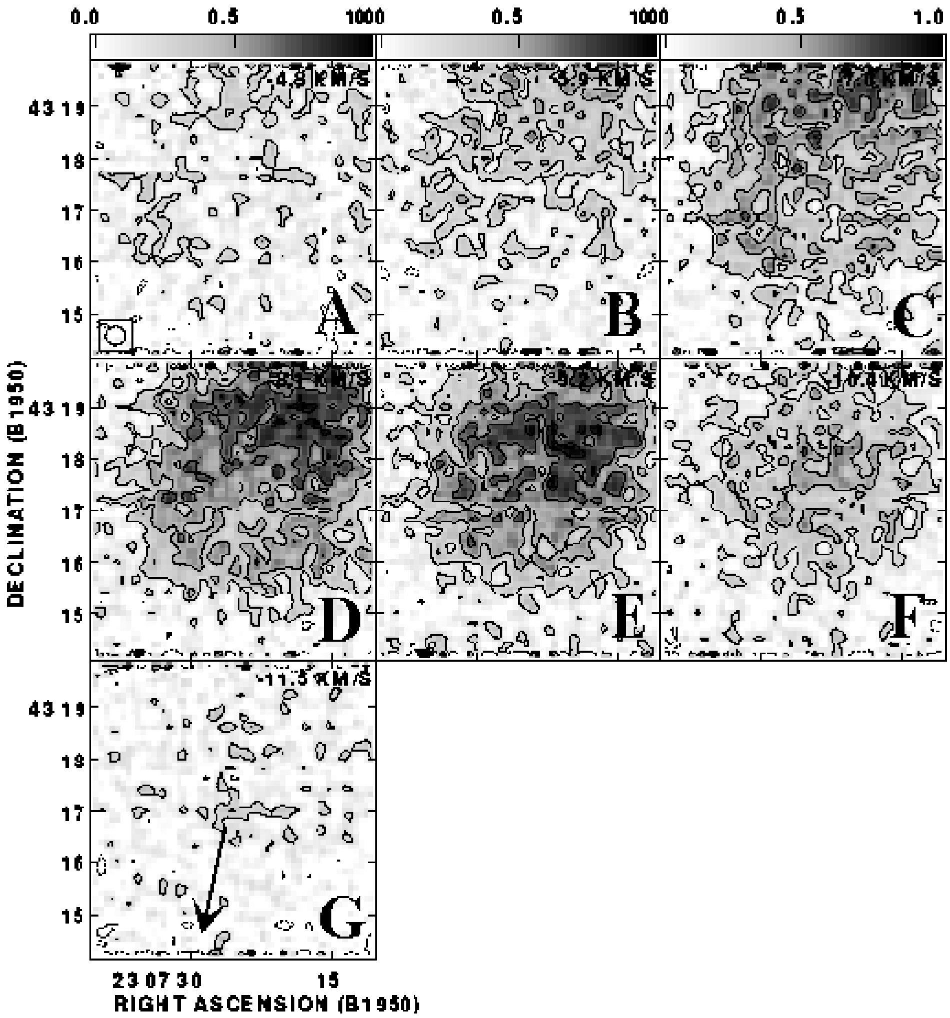

Figure 1. Maps of HCO^+ J = 3-2 transition in Comet C/1995 O1 obtained with 1000 kHz/channel spectral resolution. Panels A–G show the distribution of the ion at different velocities (corresponding to a range of topocentric radial velocities of -4.8 km s^{-1} (panel A), to -11.5 km s^{-1}, (panel G), with increments of -1.1 km s^{-1}). The darker shades of gray indicate regions of stronger emission. The emission is shown in terms of T_R^* with levels of -0.22, 0.22, 0.44, 0.66, 0.88 and 1.10 K. North is up and east is to the left. The position of the nucleus is at the center of each panel; the Sun direction is to the lower left of each panel and is denoted by an arrow in panel G. The panels are 370,432 km on a side at the comet's distance. Note that the emission in panels D and E is strongest in the anti-sunward direction and appears to travel down the tail with higher redshifts in panels C, B, and A.

if the lines are moving very quickly, as they are accelerated down the ion tail. The width of the line is controlled primarily by dynamical effects and will be explored in a later paper.

The OTF data also clearly show that the HCO^+ emission has a strong redshifted component. The spectral datacube can be split up to provide individual maps of emission for HCO^+ at different velocities. In Figure 1 are panels labeled A through G which show the maps of HCO^+ emission corresponding to different topocentric velocities. The HPBW angular resolution is 23 arcsec (22,187 km at the comet) and is shown by a circle in the lower left of panel A. As the figure shows, most of the HCO^+ emission is distributed tailward, and in fact, the strongest emission is observed at ~175,000 km anti-sunward. This distance represents the deprojected distance from the nucleus to take into account foreshortening due to the low phase angle of the comet. The redshift and tailward peak of emission was also observed in HCO^+ on other dates by Veal et al. (1997); Lovell et al. (1998); and Narayanan et al. (1997). We note that in our data the peak is not exactly along the anti-sunward direction, but appears to be at an angle of ~10 degrees east of the anti-sunward direction.

In panels C and B the emission can be seen to progress down the tail until it is only seen at the outer perimeters with a speed of -4.8 km s^{-1}. This map shows emission with a redshift of ~5.0 km s^{-1} from the cometocentric velocity. The change in velocity for HCO^+ is consistent with the ion being swept up by the solar wind and interplanetary magnetic field and accelerated away from the Sun.

To further explore the physical conditions near the inner coma, we summed three panels (D, E, and F) centered on the cometocentric velocity, shown in Figure 2. This composite map, therefore, largely traces the morphology of emission traveling within 1.1 km s^{-1} of the comet's velocity. The emission traveling at the comet's velocity may also represent the approximate location where HCO^+ is first formed, since it is rapidly swept down the tail after formation. It is important to note that even when considering emission only within 1 km s^{-1} of the comet's velocity, a significant amount of the ion is detected over 200,000 km from the nuclear position in the anti-sunward direction. Thus, it appears that a significant amount of HCO^+ may be created ~175,000 km down the tail when the comet was 0.96 AU from the Sun. We note that MHD simulations show that the ion velocities in the high density sheet of the tail, along the Sun-comet axis, are small and much smaller than velocities in the more outer regions (e.g., Wegmann et al., 1987). This might also explain why the HCO^+ ions are detected in the tail with relatively small velocities.

A more interesting feature in the data, however, is a torus-like feature surrounding a void, which is especially visible in Figure 2. We note that, among the individual panels of Figure 1, this void is seen most clearly in panel D, which may be the most appropriate map to use for setting the boundaries of the contact surface. The torus consists of an inner boundary with a void 41,000 $\pm$ 6000 km in diameter and an outer boundary with a diameter of 156,000 $\pm$ 23,000 km. If

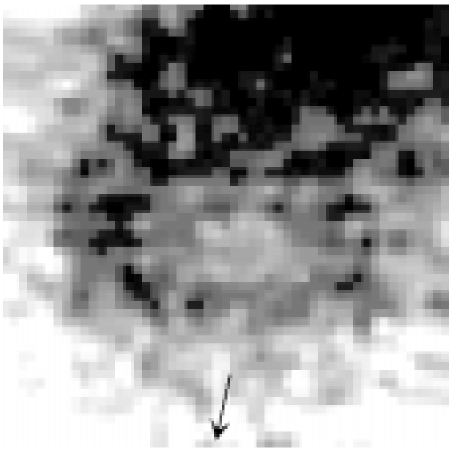

Figure 2. Sum of three maps of the HCO^+ J = 3-2 transition showing emission traveling at the comet's velocity. The direction to the Sun is denoted by an arrow. The position of the nucleus is at the center of the map. Note that there appears to be a smaller void within a larger elliptical region of decreased emission near the center of the map. This void is centered ∼11,000 km from the comet toward the Sun. In this map each side spans 295,188 km at the comet's distance.

these sizes are deprojected to include the effect of the phase angle, then the void's dimensions change to an inner boundary diameter of 55,200 ± 8100 km and an outer boundary diameter of 210,000 ± 40,400 km. This inner boundary of the torus marks a region where HCO^+ emission is reduced by a factor of two compared to emission observed 100,000 km away the outer boundary of the torus. This void is centered not exactly on the nuclear position, but at 19,200 ± 6200 km from the nucleus in the sunward direction. This decrease of HCO^+ emission near the nucleus may indicate that production or excitation of HCO^+ is inhibited, or perhaps that HCO^+ is easily destroyed in the inner coma, especially within ∼ 50,000 km of the nucleus. It is also possible that the HCO^+ emission may be quenched by the emission of electrons near the nucleus.

Interestingly, the size of the HCO^+ void coincides approximately with the that of the so-called "diamagnetic cavity" for Hale–Bopp, which is a region inside of which the magnetic field is zero (e.g., Gombosi et al., 1997–1999). Although thought to be much smaller in diameter for comet Halley, the diamagnetic cavity was predicted to be much larger for the Hale–Bopp, ∼50,000–80,000 km in diameter (Gombosi et al., 1997–1999). The inner and outer boundaries of the torus may mark the region where the electron temperature undergoes a significant transition from low to high values. Such a transition zone would have a significant impact on the production and possibly the excitation of HCO^+ in the region. In any event, the excitation conditions will not be constant throughout the coma and this may explain some of the observed structure. This will be investigated further by comparing with a detailed MHD model for the date of observation.

4. Summary

Submillimeter-wavelength maps of the HCO^+ $J = 3$-2 transition in Hale–Bopp have revealed structure near the inner coma with high angular resolution. The data show that most of the HCO^+ is observed $\sim$175,000 km from the comet anti-sunward and approximately 10 degrees eastward of the anti-sunward direction. A substantial decrease, or void, of HCO^+ emission is observed within $\sim$50,000 km of the nucleus. Thus, HCO^+ may be inhibited from production and/or excitation, or significantly destroyed near the inner coma. The void's spatial extent is also approximately the same as the predicted size of the "diamagnetic cavity" in comet Hale–Bopp predicted by MHD models (e.g., Gombosi et al., 1997–1999). Thus, the HCO^+ void may mark a transition region near the inner coma where the electron temperature is making a transition from low to very high values.

Acknowledgements

The authors thank D. Yeomans and B. Marsden for providing accurate orbital elements for the comet. M.W. acknowledges support from NSF CAREER Program Grant AST-9625360, and the Joint NASA/NSF Comet Hale–Bopp Initiative Grant NAG-5-4349. T. Uhl was supported by the NASA Grant "The Planetary Watch Program at Northern Arizona University".

References

Cravens, T. E.: 1991, 'Plasma Processes in the Inner Coma', in Newburn, Neugebauer, and Rahe (ed.), *Comets in the Post-Halley Era*, Vol. II, Kluwer Academic Publishers, Dordrecht, pp. 1211–1258.

Galeev, A. A., Sagdeev, R. Z., Shapiro, V. D., Shevchenko, V. I., and Szego, K.: 1989, 'MHD Turbulence and Particle Acceleration in a Mass-Loaded Solar Wind', *Adv. Space Res.* **9**(3), 331–336.

Gombosi, T. I., Hansen, K. C., DeZeeuw, D. L., Combi, M. R., and Powell, K. G.: 1997–1999, 'MHD Simulation of Comets: The Plasma Environment of Comet Hale–Bopp', *Earth, Moon and Planets* **79**, in press.

Ip, W.-H.: 1989, 'Ion Composition and Chemistry', *Adv. Space Res.* **9**(3), 141–150.

Larson, S. M., Hergenrother, C. W., and Brandt, J. C.: 1997, 'The Spatial and Temporal Distribution of CO^+ and CN in C/1995 O1 (Hale–Bopp)', *BAAS* **29**(3), 32.18.

Lovell, A., Schloerb, F. P., Dickens, J. E., Devries, C. H., Senay, M. C., and Irvine, W. M.: 1998, 'HCO^+ Imaging of Comet C/Hale–Bopp', *ApJ* **497**, L117–L120.

Narayanan, G., Butner, H. M., McMullin, J., and Muders, D.: 1997, *IAUC 6591*.

Veal, J. M. et al.: 1997, *IAUC 6575*.

Wegmann, R., Schmidt, H. U., Huebner, W. V., and Boice, D.C.: 1987, 'Cometary MHD and Chemistry', *A&A* **187**, 339–350.